Permeability of Cornea, Sclera, and Conjunctiva: A Literature Analysis for Drug Delivery to the Eye

MARK R. PRAUSNITZ* AND JEREMY S. NOONAN

Contribution from *Schools of Chemical Engineering and Biomedical Engineering, Georgia Institute of Technology, Atlanta, Georgia 30332-0100.*

Received June 22, 1998. Final revised manuscript received September 1, 1998.
Accepted for publication September 3, 1998.

Abstract □ The objective of this study was to collect a comprehensive database of ocular tissue permeability measurements found in a review of the literature to guide models for drug transport in the eye. Well over 300 permeability measurements of cornea, sclera, and conjunctiva, as well as corneal epithelium, stroma, and endothelium, were obtained for almost 150 different compounds from more than 40 different studies. In agreement with previous work, the corneal epithelium was shown generally to control transcorneal transport, where corneal stroma and endothelium contribute significantly only to the barrier for small, lipophilic compounds. In addition, other quantitative comparisons between ocular tissues are presented. This study provides an extensive database of ocular tissue permeabilities, which should be useful for future development and validation of models to predict rates of drug delivery to the eye.

Introduction

A significant challenge in drug delivery is the local administration of drugs to the eye.[1−3] To be effective, most drugs must penetrate across the eye's tissue barriers (e.g., cornea, sclera, and conjunctiva) to reach therapeutic targets within the globe. Often, these tissues present the rate-limiting step to effective delivery. Thus, the ability to predict rates of drug transport across ocular tissues would be a powerful tool in the development of new drugs and drug delivery strategies. Costly, time-consuming experiments using animals are usually required to determine tissue permeability. As an alternative, a few models have been developed to predict corneal permeability as a function of drug properties, such as molecular mass and partition coefficient.[4−8] However, these models have been developed using relatively small data sets, most of which were based on experiments from a single investigator's lab.

To provide models that broadly predict permeability of cornea and other ocular tissues, it would be helpful to have a database amassed from experiments conducted in many different labs that includes permeabilities for a large collection of compounds having a wide range of physicochemical properties. Such a data set would provide a resource of use to both suggest the form of theoretical models and validate their predictions.

We have collected from the literature permeability data for almost 150 different compounds for transport across cornea, sclera, and conjunctiva, as well as corneal epithelium, stroma, and endothelium. With well over 300 data points from over 40 different studies, this may represent a complete collection of all ocular tissue permeabilities published. In this study, we have used the data set to perform only a preliminary analysis. However, in ongoing work we are developing more rigorous models [9] and hope this database will similarly be of use for model development by others.

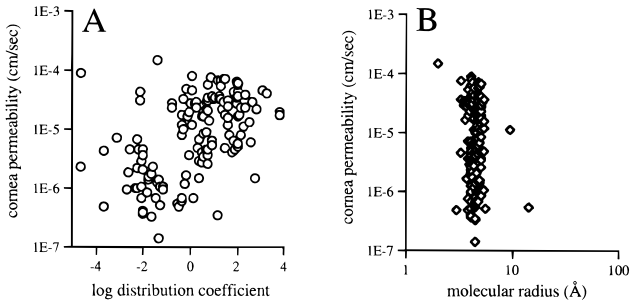

Figure 1—Permeability of cornea as a function of (A) octanol–water distribution coefficient and (B) radius of the transporting molecule. All data come from Table 1. Cornea permeability appears to be a function of the distribution coefficient.

Analytical Methods

To determine van der Waals radii of small compounds (i.e., ≪ 10 Å), the CONCORD program (Tripos, St. Louis, MO) was first used to generate three-dimensional coordinates, which were then used to compute van der Waals volumes using SAVOL3 (software provided courtesy of R. S. Pearlman, University of Texas at Austin).[10] Molecular radii were estimated from van der Waals volumes by making the imperfect assumption that all molecules have a spherical shape. Stokes−Einstein radii are reported for macromolecules, determined from experimental diffusivity data using the Stokes−Einstein equation.[11] Molecular sizes are important for determining hindrance to transport, especially for hydrophilic pathways such as through intercellular junctions and within the collagen matrix of sclera and stroma.

Octanol−water partition coefficients were determined using experimentally determined LogPstar values when available; predicted CLOGP values were used otherwise (Daylight Chemical Information Systems, Santa Fe, NM). LogPstar values come directly from experimental literature measurements, while CLOGP values are calculated on the basis of a group contribution approach generated from experimental measurements. The SPARC Multiple Property Output program (software provided courtesy of B. Carreira, University of Georgia) was used to determine the fraction of each compound that was ionized at the experimental pH. Zwitterionic charge states were considered ionized. Assuming that no charged species partition into octanol, the octanol−water

* Corresponding author. Telephone: 404-894-5135. Fax: 404-894-2866. E-mail: mark.prausnitz@che.gatech.edu.

10.1021/js9802594 CCC: $15.00
Published on Web 10/15/1998

Table 1—Permeability of Cornea

compound	M_r[a] (Da)	radius (Å)	non-ionized[b] (%)	pH	log *P*[c]	log *D*[d]	animal[e]	permeability[f] (cm/s)	ref
acebutolol	336	5.1	1	7.4	1.63	–0.74	R	1.1E–6[s]	14
acebutolol	336	5.1	2	7.65	1.63	–0.07	R	8.5E–7	15
acetazolamide	222	4.0	13	7.4	–0.26	–1.15	R	9.5E–7	16
acetazolamide	222	4.0	7	7.7	–0.26	–1.41	R	1.3E–6	17
acetazolamide	222	4.0	9	7.6	–0.26	–1.31	R	5.1E–7	18
acetazolamide der. 1[g]	284	4.4	8	7.6	0.72	–0.38	R	6.0E–7	18
acetazolamide der. 2[g]	276	4.4	4	7.6	0.87	–0.53	R	5.6E–7	18
acetazolamide der. 3[g]	236	4.1	7	7.7	–0.45	–1.60	R	2.3E–6	17
alprenolol	249	4.7	1	7.4	2.65	0.65	R	2.9E–5	14
aniline	93	3.3	100	7.4	0.92	0.92	R	3.6E–5	4
aniline der. 1[h]	150	3.8	100	7.4	–0.07	–0.07	R	3.6E–6	4
aniline der. 2[h]	135	3.7	100	7.4	0.97	0.97	R	3.2E–5	4
aniline der. 3[h]	136	3.7	100	7.4	–0.19	–0.19	R	1.7E–6	4
aniline der. 4[h]	123	3.6	100	7.4	–0.12	–0.12	R	1.7E–5	4
aniline der. 5[h]	137	3.8	100	7.4	–0.04	–0.04	R	2.0E–5	4
aniline der. 6[h]	128	3.5	100	7.4	1.96	1.96	R	3.5E–5	4
aniline der. 7[h]	137	3.8	0	7.4	1.57	1.57	R	3.1E–5	4
aniline der. 8[h]	121	3.7	99	7.4	1.94	1.94	R	2.7E–5	4
aniline der. 9[h]	135	3.9	99	7.4	2.34	2.34	R	2.4E–5	4
aniline der. 10[h]	123	3.6	100	7.4	1.04	1.04	R	3.5E–5	4
aniline der. 11[h]	107	3.5	99	7.4	1.41	1.41	R	3.0E–5	4
atenolol	266	4.7	1	7.4	–0.11	–2.11	R	1.1E–6	14
atenolol	266	4.7	1	7.65	–0.11	–2.11	R	6.8E–7	15
benzolamide	320	4.5	1	7.2	0.32	–1.68	R	3.3E–7	19
benzolamide	320	4.5	2	7.6	0.32	–1.38	R	1.4E–7	20
benzolamide	320	4.5	2	7.6	0.32	–1.38	H	1.4E–6	20
benzolamide	320	4.5	2	7.6	0.32	–1.38	R	1.4E–7	18
betaxolol	307	5.0	1	7.4	2.17	0.17	R	2.7E–5	14
bevantolol	345	5.1	4	7.65	2.65	1.25	R	5.4E–5	15
bromacetazolamide	301	4.1	1	7.6	–0.02	–2.02	R	4.2E–7	20
bromacetazolamide	301	4.1	1	7.6	–0.02	–2.02	H	3.6E–6	20
bromacetazolamide	301	4.1	1	7.6	–0.02	–2.02	R	3.6E–7	21
bromacetazolamide	301	4.1	47	5.4	–0.02	–0.34	R	6.7E–7	21
bromacetazolamide	301	4.1	1	7.6	–0.02	–2.02	R	4.0E–7	18
bromacetazolamide	301	4.1	1	7.6	–0.02	–2.02	F	2.1E–6	18
bufuralol	261	4.7	1	7.65	3.40	1.40	R	7.2E–5	15
butanol	74	3.3	100	7.5	0.82	0.82	R	7.6E–5	22
chloramphenicol	323	4.6	0	7.65	na[o]		R	6.8E–6	23
chlorzolamide	276	4.3	92	7.6	1.53	1.49	R	1.8E–5	18
cimetidine	252	4.5	61	7.4	0.35	0.14	R	7.0E–7	16
clonidine	230	4.2	0.03	7.65	1.37	–2.16	R	4.4E–5	24
clonidine	230	4.2	0.03	7.7	1.37	–2.16	R	3.1E–5	25
cocaine	303	4.8	72	7.15	2.72	2.58	R	6.1E–6	26
cortexolone	346	5.1	100	7.65	2.62	2.62	R	3.0E–5	27
corynanthine	354	5.1	17	7.7	3.01	2.24[p]	R	1.1E–5	25
cromolyn	468	5.3	0.1	7.5	1.85	–1.15	R	1.1E–6	22
cyclophosphamide	261	4.3	na	7.65	0.80	na	R	1.1E–5	28
cyclosporin	1201	9.5	100	7.65			R	1.1E–5	29
deoxycorticosterone	330	5.0	100	7.65	3.25	3.25	R	4.0E–5	27
2-deoxyglucose	165	3.8	100	7.65	–3.12	–3.12	R	7.4E–6	29
2-deoxyglucoseder. 1[i]	204	4.2	100	7.65	–2.25	–2.25	R	2.2E–6	29
2-deoxyglucoseder. 2[i]	192	4.1	100	7.65	–2.07	–2.07	R	2.9E–6	29
2-deoxyglucoseder. 3[i]	206	4.2	100	7.65	–1.67	–1.67	R	1.8E–6	29
2-deoxyglucoseder. 4[i]	178	4.0	100	7.65	–2.60	–2.60	R	4.6E–6	29
dexamethasone	392	5.2	100	7.65	1.49	1.49	R	5.0E–6	27
dexamethazone acetate	434	5.3	100	7.65	2.02	2.02	R	3.7E–5	27
2,5-dimethoxyaniline	153	3.9	100	7.4	1.25	1.25	R	3.3E–5	4
edetic acid (EDTA)	292	4.6	5e-6	7.5	–4.69	–11.99	R	2.1E–6	22
ethanolamine	61	3.0	0.4	7.4	–1.30	–3.69	R	5.0E–7	4
ethoxzolamide	258	4.3	95	7.65	2.02	2.00	R	4.4E–5	30
ethoxzolamide	258	4.3	95	7.6	2.02	2.00	H	3.6E–5	20
ethoxzolamide	258	4.3	95	7.6	2.02	2.00	R	5.6E–5	20
ethoxzolamide	258	4.3	95	7.6	2.02	2.00	R	5.6E–5	18
ethoxzolamide der. 1[j]	214	4.0	92	7.65	1.23	1.19[q]	R	3.6E–5	30
ethoxzolamide der. 2[j]	230	4.1	88	7.65	0.98	0.92[q]	R	5.6E–6	30
ethoxzolamide der. 3[j]	249	4.1	6	7.65	3.08	1.86[q]	R	4.3E–5	30
ethoxzolamide der. 4[j]	283	4.2	4	7.65	3.70	2.30[q]	R	3.9E–5	30
ethoxzolamide der. 5[j]	229	4.1	12	7.65	1.301	0.38[q]	R	6.7E–6	30
ethoxzolamide der. 6[j]	259	4.2	3	7.65	2.42	0.90[q]	R	6.6E–6	30
ethoxzolamide der. 7[j]	274	4.4	11	7.65	1.34	0.38[q]	R	1.5E–6	30
ethoxzolamide der. 8[j]	320	4.7	10	7.65	4.06	3.06[q]	R	4.7E–5	30
ethoxzolamide der. 9[j]	271	4.3	4	7.65	2.08	0.68[q]	R	4.7E–6	30

Table 1 (Continued)

compound	M_r[a] (Da)	radius (Å)	non-ionized[b] (%)	pH	log *P*[c]	log *D*[d]	animal[e]	permeability[f] (cm/s)	ref
fluorometholone	376	5.1	100	7.65	2.01	2.01	R	1.7E–5	27
flurbiprofen	244	4.4	0.1	7.4	3.75	0.75	R	2.1E–5	16
flurbiprofen amide	243	4.4	100	7.4	2.79	2.79	R	2.2E–5	16
glycerol	92	3.3	100	7.5	–2.19	–2.19	R	4.5E–6	22
hydrocortisone	362	5.1	100	7.65	0.54	0.54	R	8.5E–6	27
hydrocortisone	362	5.1	100	7.5	0.54	0.54	R	3.5E–6	22
ibuprofen	206	4.4	0.1	7.65	3.68	0.68	R	2.2E–5	29
indomethacin	358	4.9	0.1	7.6	4.18	1.18	R	6.9E–5	32
inulin	5000	14.0	100	7.0			R	5.5E–7	33
labetalol	328	5.0	2	7.4	2.50	0.80	R	1.4E–5	14
levobunolol	291	4.8	1	7.4	2.26	0.26	R	2.9E–5	16
levobunolol	291	4.8	1	7.4	2.26	0.26	R	2.3E–5	14
levobunolol	291	4.8	2	7.65	2.26	0.56	R	1.7E–5	15
mannitol	182	4.0	100	7.5	–4.67	–4.67	R	2.4E–6	22
mannitol	182	4.0	100	7.5	–4.67	–4.67	R	9.1E–5	22
methazolamide	236	4.1	34	7.6	na		R	2.6E–6	20
methazolamide	236	4.1	34	7.6	na		H	4.9E–6	20
methazolamide	236	4.1	31	7.65	na		R	4.2E–6	29
methazolamide	236	4.1	14	8.6	na		R	1.9E–6	21
methazolamide	236	4.1	19	5.0	na		R	7.3E–6	21
methazolamide	236	4.1	34	7.6	na		R	2.6E–6	18
methazolamide der.[k]	194	3.8	0.9	7.6	na		R	7.8E–7	18
methylenedianiline	198	4.3	99	7.4	1.61	1.60	R	2.5E–5	4
metoprolol	267	4.8	1	7.4	1.20	–0.80	R	2.8E–5	14
metoprolol	267	4.8	1	7.65	1.20	–0.80	R	2.4E–5	15
MK-927	338	4.7	1	5.2	–0.03	–2.03	R	4.6E–6	19
nadolol	309	4.9	1	7.4	0.23	–1.77	R	1.4E–6	14
nadolol	309	4.9	0.3	7.0	0.23	–2.29	R	6.9E–6	33
nadolol	309	4.9	1	7.65	0.23	–1.77	R	1.6E–6	15
nadolol diacetate	393	5.3	2	7.65	2.02	0.32	R	4.8E–6	29
oxprenolol	265	4.7	1	7.4	1.69	–0.31	R	3.2E–5	14
oxprenolol	265	4.7	2	7.65	1.69	–0.01	R	2.8E–5	15
penbutolol	291	4.9	0.2	7.0	4.04	1.34	R	2.2E–5	33
penbutolol	291	4.9	1	7.65	4.04	2.04	R	6.0E–5	15
phenylephrine	167	4.0	1	7.7	–0.72	–2.72[p]	R	9.4E–7	25
pilocarpine	208	4.3	53	7.65	0.74	0.46	R	1.7E–5	23
pilocarpine	208	4.3	53	7.65	0.74	0.46	R	2.8E–6	34
pilocarpine	208	4.3	11	6.6	0.74	–0.22	C	1.2E–6	35
pindolol	248	4.6	1	7.4	1.67	–0.33	R	1.0E–5	14
prednisolone	360	5.0	100	7.65	0.72	0.72	R	3.7E–6	27
prednisolone	360	5.0	100	7.4	0.72	0.72	R	4.5E–6	16
prednisolone	360	5.0	100	7.4	0.72	0.72	R	2.7E–6	36
prednisolone acetate	402	5.2	100	7.65	1.26	1.26	R	3.3E–5	27
procaine	236	4.5	1.3	7.15	2.38	0.49	R	4.2E–6	26
progesterone	314	5.0	100	7.65	3.78	3.78	R	2.0E–5	27
progesterone	314	5.0	100	7.5	3.78	3.78	R	1.8E–5	22
propranolol	259	4.7	1	7.5	2.75	0.75	R	3.1E–5	22
propranolol	259	4.7	1	7.4	2.75	0.75	R	3.4E–5	14
propranolol	259	4.7	0.2	7.0	2.75	0.05	R	4.6E–5	33
propranolol	259	4.7	1	7.65	2.75	0.75	R	5.8E–5	15
rauwolfine	314	4.9	3	7.7	2.22	0.70[p]	R	9.2E–6	25
SKF 72223[l]	193	4.2	33	7.7	0.32	–0.16[p]	R	4.9E–5	25
SKF 86466[l]	196	4.2	12	7.7	2.40	1.48[p]	R	7.1E–5	25
SKF 86607[l]	191	4.0	54	7.7	0.30	0.03[p]	R	7.9E–5	25
sotalol	272	4.6	2	7.4	0.23	–1.47	R	7.0E–7	14
sotalol	272	4.6	0.3	7.65	0.23	–2.30	R	1.0E–6	15
sucrose	342	4.8	100	7.0	–3.70	–3.70	R	4.3E–6	33
sulfacetamide	214	4.1	2	7.65	–0.93	–2.62	R	1.9E–6	23
sulfacetamide	214	4.1	4	7.4	–0.93	–2.32	R	1.0E–6	16
sulfanilamide	172	3.8	100	7.4	–0.50	–0.50	R	5.0E–7	4
sulfonamide der. 1[m]	229	4.4	0	7.0	na		R	3.6E–6	19
sulfonamide der. 2[m]	223	3.9	40	7.65	0.74	0.34	R	3.0E–6	29
sulfonamide der. 3[m]	206	4.0	100	7.7	1.94	1.94	R	6.5E–5	17
sulfonamide der. 4[m]	192	3.8	99	7.7	1.26	1.26	R	5.5E–5	17
testosterone	288	4.8	100	7.65	3.22	3.22	R	4.2E–5	27
tetracaine	264	4.7	12	7.15	3.65	2.73	R	1.5E–6	26
thiadiazole der. 1[n]	313	4.5	87	7.65	1.710	1.65[r]	R	7.9E–6	37
thiadiazole der. 2[n]	348	4.6	95	7.65	2.532	2.51[r]	R	1.3E–5	37
thiadiazole der. 3[n]	348	4.6	95	7.65	2.152	2.13[r]	R	8.3E–6	37
thiadiazole der. 4[n]	343	4.6	88	7.65	1.946	1.89[r]	R	4.5E–6	37
thiadiazole der. 5[n]	343	4.6	79	7.65	2.112	2.01[r]	R	5.2E–6	37
thiadiazole der. 6[n]	329	4.5	65	7.65	1.327	1.14[r]	R	3.5E–7	37

Table 1 (Continued)

compound	M_r[a] (Da)	radius (Å)	non-ionized[b] (%)	pH	log *P*[c]	log *D*[d]	animal[e]	permeability[f] (cm/s)	ref
thiadiazole der. 7[n]	331	4.5	94	7.65	1.887	1.86[r]	R	6.4E–6	37
thiadiazole der. 8[n]	331	4.5	92	7.65	1.776	1.74[r]	R	4.1E–6	37
thiadiazole der. 9[n]	356	4.7	52	7.65	2.314	2.03[r]	R	5.8E–6	37
timolol	316	4.8	1	7.4	1.61	–0.39	R	1.2E–5	14
timolol	316	4.8	1	7.4	1.61	–0.39	R	1.8E–5	38
timolol	316	4.8	1	7.0	1.61	–0.39	R	8.0E–6	33
timolol	316	4.8	3	7.65	1.61	0.09	R	1.2E–5	15
tobramycin	467	5.5	na	7.65	–7.32	na	R	5.2E–7	23
triamcinolone acetonide	435	5.3	100	7.65	1.60	1.60	R	1.2E–5	27
triamcinolone acetonide	435	5.3	100	7.5	1.60	1.60	R	1.6E–5	22
trichlormethazolamide	339	4.4	42	7.5	na		R	6.5E–6	19
trichlormethazolamide	339	4.4	37	7.6	na		R	1.0E–5	21
trichlormethazolamide	339	4.4	96	6.0	na		R	2.4E–5	21
trichlormethazolamide	339	4.4	37	7.6	na		R	1.1E–5	18
trifluormethazolamide	290	4.3	42	7.6	na		R	3.9E–6	18
water	18	2.0	100	7.5	–1.38	–1.38	R	1.5E–4	22
yohimbine	354	5.1	17	7.7	2.87	2.10[p]	R	1.8E–5	25
α-yohimbine	354	5.1	17	7.7	2.92	2.15[p]	R	2.3E–5	25

[a] Molecular mass (or average molecular mass). [b] Percent of molecules non-ionized at experimental pH. [c] Octanol–water partition coefficient, *P*. Partition coefficients were not calculated for ions and macromolecules, since they are assumed not to partition into the lipid phase. [d] Octanol–water distribution coefficient, *D*, determined at experimental pH. [e] Source of tissue: rabbit (R); human (H); cow (C); cat (F). [f] All permeability measurements were made in vitro. [g] Acetazolamide derivatives: 2-benzoylamino-1,3,4-thiadiazole 5-sufonamide (1); 2-isopentenyl amino 1,3,4-thiadiazole-5-sulfonamide (2); *N*-methylacetazolamide (3). [h] Para-substituted aniline derivatives: aminoacetanilide (1); aminoacetophenone (2); aminobenzamide (3); aminobenzyl alcohol (4); aminophenylethanol (5); chloroaniline (6); ethoxyaniline (7); ethylaniline (8); isopropylaniline (9); methoxyaniline (10); toluidine (11). [i] 2-Deoxyglucose derivatives with 1-α substitution: cyclopropyl (1); ethyl (2); isopropyl (3); methyl (4). [j] Substituted 2-benzothiazole-sulfonamide derivatives: no substitution (1); 6-hydroxy (2); 6-chloro (3); 4,6-dichloro (4); 6-amino (5); 6-nitro (6); 6-hydroxyethoxy- (7); 6-benzyloxy (8); 6-acetamido (9). [k] 5-Imino-4-methyl-1,3,4 thiadiazoline-2-sulfonamide. [l] SKF 72223, 5,8-Dimethoxy-1,2,3,4-tetrahydroisoquinoline; SKF 86466, 6-chloro-3-methyl-2,3,4,5-tetrahydro-1*H*-3-benzazepine); SKF 86607, [1,2,3]thiadiazolo[5,4-*h*]–6,7,8,9-tetrahydroisoquinoline). [m] Substituted sulfonamide derivatives: quaternary ammonium (1); 2-benzimidazole (2); 4-chloro-*N*-methylbenzene (3); 4-chlorobenzene (4). [n] 6-Sulfonamido-3-substituted-3*H*-1,3,4-thiadiazolo[2,3-*C*]-1,2,4-thiadiazole: no substitution (1); 3-chloro (2); 4-chloro (3); 3-methoxy (4); 4-methoxy (5); 4-hydroxy (6); 3-fluoro (7); 4-fluoro (8); 4-dimethylamino (9). [o] Data not available. [p] log *D* was obtained from ref 25, and corresponding log *P* was calculated from it. [q] log *D* was obtained from ref 30, and corresponding log *P* was calculated from it. [r] log *D* was obtained from ref 37, and corresponding log *P* was calculated from it. [s] Read as 1.1×10^{-6}.

Table 2—Permeability of Corneal Stroma

compound	M_r[a] (Da)	radius (Å)	non-ionized[b] (%)	pH	log *P*[c]	log *D*[d]	animal[e]	permeability[f] (cm/s)	ref
acebutolol	336	5.1	2	7.65	1.63	–0.09	R	3.0E–5	15
albumin, serum	65 000	35	0	7.0			R	1.4E–7	39
atenolol	266	4.7	1	7.65	–0.11	–2.11	R	3.3E–5	15
bevantolol	345	5.1	4	7.65	2.65	1.25	R	3.4E–5	15
bufuralol	261	4.7	1	7.65	3.40	1.40	R	4.0E–5	15
clonidine	230	4.2	0.03	7.7	1.37	–2.16	R	4.9E–5	25
corynanthine	354	5.1	17	7.7	3.01	2.24[i]	R	3.2E–5	25
hemoglobin	64 500	31	0	na[h]			O	5.7E–7	40
IgG	140 000	50	0	7.4			R	8.0E–9*	41
metoprolol	267	4.8	1	7.65	1.20	–0.80	R	3.4E–5	15
oxprenolol	265	4.7	2	7.65	1.69	–0.01	R	3.7E–5	15
phenylephrine	167	4.0	1	7.7	–0.72	–2.72[i]	R	5.8E–5	25
propranolol	259	4.7	1	7.65	2.75	0.75	R	3.5E–5	15
rauwolfine	314	4.9	3	7.7	2.22	0.70[i]	R	3.6E–5	25
SKF 72223[g]	193	4.2	33	7.7	0.32	–0.16[i]	R	4.2E–5	25
SKF 86466[g]	196	4.2	12	7.7	2.40	1.48[i]	R	5.7E–5	25
SKF 86607[g]	191	4.0	54	7.7	0.30	0.03[i]	R	5.3E–5	25
yohimbine	354	5.1	17	7.7	2.87	2.10[i]	R	3.9E–5	25
α-yohimbine	354	5.1	17	7.7	2.92	2.15[i]	R	3.7E–5	25

[a] Molecular mass (or average molecular mass). [b] Percent of molecules non-ionized at experimental pH. [c] Octanol–water partition coefficient, *P*. Partition coefficients were not calculated for macromolecules, since they are assumed not to partition into the lipid phase. [d] Octanol–water distribution coefficient, *D*, determined at experimental pH. [e] Source of tissue: rabbit (R); ox (O). [f] All permeability measurements were made in vitro, except the one followed by an asterix (*), which was made in vivo. [g] SKF 72223, 5,8-dimethoxy-1,2,3,4-tetrahydroisoquinoline; SKF 86466, 6-chloro-3-methyl-2,3,4,5-tetrahydro-1*H*-3-benzazepine); SKF 86607, [1,2,3]thiadiazolo[5,4-h]-6,7,8,9-tetrahydroisoquinoline). [h] Data not available. [i] log *D* was obtained from ref 25, and corresponding log *P* was calculated from it.

distribution coefficient was calculated as the product of the partition coefficient and the fraction un-ionized. Distribution coefficients, which are a measure of lipophilicity, are important for determining the ability of molecules to access transmembrane pathways across the corneal epithelium, endothelium, and conjunctiva.

The above physicochemical properties have been determined using a number of different software packages, some of which may not be easily available to others. We believe that the calculation methods used in this study are robust, but there are other methods of calculating molecular radius and distribution coefficient that are also acceptable. Given the scatter in the data presented here, small differences in calculated physicochemical properties are probably not significant and the choice of calculation method is flexible.

For some compounds, no distribution coefficient is provided (i.e., in Tables 1−7), either because necessary data were not available or because the coefficient was assumed to be zero; ions and macromolecules were assumed not to partition into the lipid phase. As a result, graphs with distribution coefficient on the abscissa contain most, but not all of the compounds that appear on their corresponding graphs with molecular radius on the abscissa (e.g.,

Table 3—Permeability of Corneal Endothelium

compound	M_r[a] (Da)	radius (Å)	non-ionized[b] (%)	pH	log P[c]	log D[d]	animal[e]	permeability[f] (cm/s)	ref
albumin, serum	65 000	35	0	7.4			R	8.3E–9*	41
arabinose	150	3.7	100	na[g]	–2.86	–2.86	R	1.9E–5	42
arginine	174	4.0	5E-6	7.5	–4.62	–15.31	R	8.3E–6	43
aspartate ion	132	3.4	0	7.5			R	1.1E–5	43
bicarbonate ion	61	2.5	0	na			R	2.1E–5	44
chloride ion	35	1.8	0	na			R	2.3E–5	44
chloride ion	35	1.8	0	7.3			R	2.8E–5	45
chloride ion	35	1.8	0	na			R	2.7E–5	46
dextran	16 000	34	100	7.3			R	7.5E–7	45
dextran	75 000	66	100	7.3			R	1.1E–7	45
fluorescein	332	4.8	0	na	2.48	–4.28	R	5.0E–6	42
fluorescein	332	4.8	0	7.4	2.48	–4.28	R	5.1E–6*	47
fluorescein	332	4.8	0	7.4	2.48	–4.28	H	3.0E–6*	47
inulin	5000	14	100	7.3			R	1.4E–6	45
inulin	5000	14	100	7.3			R	1.3E–6	48
lactate ion	89	3.1	0	na			R	2.8E–5	42
mannitol	182	4.0	100	7.3	–4.67	–4.67	R	9.2E–6	45
phosphate ion	95	2.6	0	na			R	4.4E–6	44
poly(vinylpyrrolidone)	45 000	50	na	7.3			R	3.8E–7	45
rubidium ion	85	1.5	0	na			R	3.4E–5	46
sodium ion	23	1.0	0	na			R	1.9E–5	44
sodium ion	23	1.0	0	na			R	2.0E–5*	49
sucrose	342	4.8	100	7.3	–3.70	–3.70	R	5.8E–6	45
sucrose	342	4.8	100	7.3	–3.70	–3.70	R	6.4E–6	48
sucrose	342	4.8	100	7.5	–3.70	–3.70	R	5.6E–6	43
thiocyanate ion	58	2.6	0	na			R	2.5E–5	46
urea	60	2.8	100	7.3	–2.11	–2.11	R	2.1E–5	48
urea	60	2.8	100	7.5	–2.11	–2.11	R	1.8E–5	43
water	18	2.0	100	7.3	–1.38	–1.38	R	1.7E–4	48

[a] Molecular mass (or average molecular mass). [b] Percent of molecules non-ionized at experimental pH. [c] Octanol–water partition coefficient, *P*. Partition coefficients were not calculated for ions and macromolecules, since they are assumed not to partition into the lipid phase. [d] Octanol–water distribution coefficient, *D*, determined at experimental pH. [e] Source of tissue: rabbit (R); human (H). [f] All permeability measurements were made in vitro, except those followed by an asterix (*), which were made in vivo. [g] Data not available.

Table 4—Permeability of Corneal Epithelium-plus-Stroma

compound	M_r[a] (Da)	radius (Å)	non-ionized[b] (%)	pH	log P[c]	log D[d]	animal[e]	permeability[f] (cm/s)	ref
acebutolol	336	5.1	2	7.65	1.63	–3.08	R	9.7E–7	15
atenolol	266	4.7	1	7.65	–0.11	–2.11	R	6.4E–7	15
bevantolol	345	5.1	4	7.65	2.65	1.25	R	4.5E–5	15
bufuralol	261	4.7	1	7.65	3.40	1.40	R	4.8E–5	15
clonidine	230	4.2	0.03	7.7	1.37	–2.16	R	3.0E–5	25
corynanthine	354	5.1	17	7.7	3.01	2.24[h]	R	1.1E–5	25
metoprolol	267	4.8	1	7.65	1.20	–0.80	R	2.3E–5	15
oxprenolol	265	4.7	2	7.65	1.69	–0.01	R	2.6E–5	15
phenylephrine	167	4.0	1	7.7	–0.72	–2.72[h]	R	1.3E–6	25
propranolol	259	4.7	1	7.65	2.75	0.75	R	3.9E–5	15
rauwolfine	314	4.9	3	7.7	2.22	0.70[h]	R	9.9E–6	25
SKF 72223[g]	193	4.2	33	7.7	0.32	–0.16[h]	R	4.9E–5	25
SKF 86466[g]	196	4.2	12	7.7	2.40	1.48[h]	R	6.7E–5	25
SKF 86607[g]	191	4.0	54	7.7	0.30	0.03[h]	R	6.6E–5	25
yohimbine	354	5.1	17	7.7	2.87	2.10[h]	R	1.8E–5	25
α-yohimbine	354	5.1	17	7.7	2.92	2.15[h]	R	2.3E–5	25

[a] Molecular mass (or average molecular mass). [b] Percent of molecules nonionized at experimental pH. [c] Octanol–water partition coefficient, *P*. [d] Octanol–water distribution coefficient, *D*, determined at experimental pH. [e] Source of tissue: rabbit (R). [f] All permeability measurements were made in vitro. [g] SKF 72223, 5,8-dimethoxy-1,2,3,4-tetrahydroisoquinoline; SKF 86466, 6-chloro-3-methyl-2,3,4,5-tetrahydro-1*H*-3-benzazepine); SKF 86607, [1,2,3]thiadiazolo[5,4-*h*]-6,7,8,9-tetrahydroisoquinoline). [h] log *D* was obtained from ref 25, and corresponding log *P* was calculated from it.

Figure 1B versus Figure 1A). An effect of this is that distribution coefficient graphs do not include data for small ions or macromolecules and as a result contain data only for compounds of approximately the same molecular radius (3.5−5.5 Å). This simplifies analysis, since it removes concerns about differences due to molecular size between partitioning into liquid octanol versus the structured lipid bilayers found in tissue, which octanol is supposed to simulate.

Permeability values were obtained directly from the papers that reported them or calculated using information provided in the papers. No judgments were made about the "quality" of data; all reported data were used and accepted as correct. Exceptions were permeability values for compounds reported to be transported actively or to be chemically altered during transport (e.g., prodrugs); such data are not included in this analysis. All studies were performed at a temperature between 33 and 37 °C or at "body" temperature when in vivo studies were used. No adjustments to the data on the basis of different animal tissue sources have been made (e.g., normalize permeability on the basis of tissue thickness), since these adjustments would only produce relatively small corrections to the data.

Table 5—Permeability of Corneal Endothelium-plus-Stroma

compound	M_r[a] (Da)	radius (Å)	non-ionized[b] (%)	pH	log P[c]	log D[d]	animal[e]	permeability[f] (cm/s)	ref
acebutolol	336	5.1	2	7.65	1.63	–0.07	R	9.3E–6	15
acetazolamide	222	4.0	9	7.6	–0.26	–1.31	R	9.7E–6	18
acetazolamide der. 1[g]	284	4.4	8	7.6	0.72	–0.38	R	8.3E–6	18
acetazolamide der. 2[g]	276	4.4	4	7.6	0.87	–0.53	R	9.7E–6	18
atenolol	266	4.7	1	7.65	–0.11	–2.11	R	1.6E–5	15
benzolamide	320	4.5	2	7.6	0.32	–1.38	H	1.1E–5	20
benzolamide	320	4.5	2	7.6	0.32	–1.38	R	9.7E–6	18
bevantolol	345	5.1	4	7.65	2.65	1.25	R	3.4E–5	15
bromacetazolamide	301	4.1	1	7.6	–0.02	–2.02	H	1.1E–5	20
bromacetazolamide	301	4.1	47	5.4	–0.02	–0.34	R	2.1E–5	21
bromacetazolamide	301	4.1	1	7.6	–0.02	–2.02	R	8.7E–6	21
bromacetazolamide	301	4.1	1	7.6	–0.02	–2.02	R	9.7E–6	18
bromacetazolamide	301	4.1	1	7.6	–0.02	–2.02	F	2.4E–5	18
bufuralol	261	4.7	1	7.65	3.40	1.40	R	4.0E–5	15
chlorzolamide	276	4.3	92	7.6	1.53	1.49	R	3.6E–5	18
clonidine	230	4.2	0.03	7.7	1.37	–2.16	R	4.7E–5	25
corynanthine	354	5.1	17	7.7	3.01	2.24[k]	R	3.1E–5	25
ethoxzolamide	258	4.3	95	7.6	2.02	2.00	H	3.6E–5	20
ethoxzolamide	258	4.3	95	7.6	2.02	2.00	R	3.9E–5	18
levobunolol	291	4.8	2	7.65	2.26	0.56	R	2.5E–5	15
methazolamide	236	4.1	34	7.6	na[j]		H	2.2E–5	20
methazolamide	236	4.1	19	5.0	na		R	2.9E–5	21
methazolamide	236	4.1	19	8.6	na		R	2.2E–5	21
methazolamide	236	4.1	34	7.6	na		R	1.8E–5	18
methazolamide der.[h]	194	3.8	0.9	7.6	na		R	1.7E–5	18
metoprolol	267	4.8	1	7.65	1.20	–0.80	R	2.8E–5	15
nadolol	309	4.9	1	7.65	0.23	–1.77	R	1.5E–5	15
oxprenolol	265	4.7	2	7.65	1.69	–0.01	R	3.1E–5	15
penbutolol	291	4.9	1	7.65	4.04	2.04	R	2.9E–5	15
phenylephrine	167	4.0	1	7.7	–0.72	–2.72[k]	R	2.1E–5	25
propranolol	259	4.7	1	7.65	2.75	0.75	R	3.1E–5	15
rauwolfine	314	4.9	3	7.7	2.22	0.70[k]	R	2.3E–5	25
SKF 72223[i]	193	4.2	33	7.7	0.32	–0.16[k]	R	3.9E–5	25
SKF 86466[i]	196	4.2	12	7.7	2.40	1.48[k]	R	5.3E–5	25
SKF 86607[i]	191	4.0	54	7.7	0.30	0.03[k]	R	5.4E–5	25
sotalol	272	4.6	0.3	7.65	0.23	–2.30	R	1.8E–5	15
timolol	316	4.8	3	7.65	1.61	0.09	R	2.6E–5	15
trichlormethazolamide	339	4.4	96	6.0	0.47	0.46	R	4.0E–5	21
trichlormethazolamide	339	4.4	37	7.6	0.47	0.04	R	3.7E–5	21
trichlormethazolamide	339	4.4	37	7.6	0.47	0.04	R	3.9E–5	18
trifluormethazolamide	290	4.3	42	7.6	na		R	1.8E–5	18
yohimbine	354	5.1	17	7.7	2.87	2.10[k]	R	3.7E–5	25
α-yohimbine	354	5.1	17	7.7	2.92	2.15[k]	R	3.8E–5	25

[a] Molecular mass (or average molecular mass). [b] Percent of molecules non-ionized at experimental pH. [c] Octanol–water partition coefficient, P. [d] Octanol–water distribution coefficient, D, determined at experimental pH. [e] Source of tissue: rabbit (R); human (H); cat (F). [f] All permeability measurements were made in vitro. [g] Acetazolamide derivatives: 2-benzoylamino-1,3,4-thiadiazole 5-sufonamide (1); 2-isopentenyl amino 1,3,4-thiadiazole-5-sulfonamide (2). [h] 5-Imino-4-methyl-1,3,4 thiadiazoline-2-sulfonamide. [i] SKF 72223, 5,8-dimethoxy-1,2,3,4-tetrahydroisoquinoline; SKF 86466, 6-chloro-3-methyl-2,3,4,5-tetrahydro-1*H*-3-benzazepine); SKF 86607, [1,2,3]thiadiazolo[5,4-*h*]-6,7,8,9-tetrahydroisoquinoline). [j] Data not available. [k] log D was obtained from ref 25, and corresponding log P was calculated from it.

Results and Discussion

To provide a comprehensive database of the permeability of ocular tissues, we performed an analysis of literature data, which is summarized in Tables 1−7. Included in these tables are permeability data on the cornea, sclera, and conjunctiva, and also on the different layers of the cornea, including corneal stroma, endothelium, endothelium-plus-stroma, and epithelium-plus-stroma. Most molecules studied were relatively small (i.e., $r \ll 10$ Å), but some macromolecules were included. Compounds having a broad range of lipophilicities were available, as shown by distribution coefficients spanning almost 9 orders of magnitude. Most data were collected with rabbit tissue, but other sources were used too. The data listed in the tables are shown graphically in Figures 1−7.

Permeability of Cornea—Figure 1A shows the dependence of corneal permeability on the octanol−water distribution coefficient of the transported molecule. Although there is considerable scatter in the data, there is a general trend indicating that permeability increases with increasing distribution coefficient. This trend is expected both from previous experimental studies (e.g., those listed in Table 1) and from theoretical predictions.[6] In contrast, there is no apparent dependence of corneal permeability on molecular radius for the compounds tested (Figure 1B). This is potentially deceiving, because no data on macromolecules are included in the graph; permeability values for macromolecules are not available in the literature because cornea provides such a great barrier that compounds larger than about 10 Å generally cannot cross at measurable rates.[51] Combined, this yields the assertion that corneal permeability is a function of both distribution coefficient and molecular size.

This result can be further analyzed based on an understanding of corneal anatomy. The cornea contains three primary layers, which are stacked sequentially from the outer to inner surface: epithelium, stroma, and endothelium.[2,12] In the human eye, the epithelium contains 5−7

Table 6—Permeability of Sclera

compound	M_r[a] (Da)	radius (Å)	non-ionized[b] (%)	pH	log P[c]	log D[d]	animal[e]	permeability[f] (cm/s)	ref
albumin, serum	65 000	35	0	7.3			C	1.3E–7	50
benzolamide	320	4.5	2	7.6	0.32	–1.38	R	2.0E–5	20
benzolamide	320	4.5	2	7.6	0.32	–1.38	H	1.5E–5	20
bromacetazolamide	301	4.1	1	7.6	–0.02	–2.02	H	2.0E–5	20
dextran-10	10 000	27	100	7.4			H	6.2E–6	13
dextran-40	40 000	50	100	7.4			H	4.3E–6	13
dextran-70	70 000	64	100	7.4			H	1.9E–6	13
ethoxzolamide	258	4.3	95	7.6	2.02	2.00	R	2.5E–5	20
ethoxzolamide	258	4.3	95	7.6	2.02	2.00	H	3.8E–5	20
5-fluorouracil	130	3.3	8	7.4	–0.97	–2.07	H	4.4E–5	13
hemoglobin	64 500	31	0	7.3			C	3.6E–7	50
hydrocortisone	362	5.1	100	7.3	0.54	0.54	C	6.5E–6	50
inulin	5000	14	100	7.3			C	1.9E–6	50
inulin	5000	14	100	7.4			H	9.0E–6	13
inulin	5000	14	100	7.0			R	2.5E–6	33
methazolamide	236	4.1	34	7.6	na[g]		R	3.7E–5	20
methazolamide	236	4.1	34	7.6	na		H	3.0E–5	20
nadolol	309	4.9	0.03	7.0	0.23	–2.29	R	3.9E–5	33
penbutolol	291	4.9	0.02	7.0	4.04	1.34	R	7.1E–5	33
penicillin G	333	4.8	1e-4	7.3	1.70	–4.14	C	6.6E–6	50
pilocarpine	208	4.3	34	7.3	0.74	0.27	C	1.3E–5	50
propranolol	259	4.7	0.2	7.0	2.75	0.05	R	5.8E–5	33
sodium ion	23	1.0	0	7.3			C	4.6E–5	50
sucrose	342	4.8	100	7.4	–3.70	–3.70	H	2.2E–5	13
sucrose	342	4.8	100	7.0	–3.70	–3.70	R	4.2E–5	33
thiocyanate ion	58	2.6	0	7.3			C	4.5E–5	50
timolol	316	4.8	1	7.0	1.61	–0.39	R	4.1E–5	33

[a] Molecular mass (or average molecular mass). [b] Percent of molecules nonionized at experimental pH. [c] Octanol–water partition coefficient, *P*. Partition coefficients were not calculated for ions and macromolecules, since they are assumed not to partition into the lipid phase. [d] Octanol–water distribution coefficient, *D*, determined at experimental pH. [e] Source of tissue: rabbit (R); human (H); cow (C). [f] All permeability measurements were made in vitro. [g] Data not available.

Table 7—Permeability of Conjunctiva

compound	M_r[a] (Da)	radius (Å)	non-ionized[b] (%)	pH	log P[c]	log D[d]	animal[e]	permeability[f] (cm/s)	ref
acebutolol	336	5.1	1	7.4	1.63	–0.37	R	5.0E–5	14
alprenolol	249	4.7	1	7.4	2.65	0.65	R	2.4E–5	14
atenolol	266	4.7	1	7.4	–0.11	–2.11	R	5.2E–5	14
betaxolol	307	5.0	1	7.4	2.17	0.17	R	4.2E–5	14
inulin	5000	14	100	7.0			R	3.8E–6*	33
labetalol	328	5.0	2	7.4	2.50	0.80	R	6.0E–5	14
levobunolol	291	4.8	1	7.4	2.26	0.26	R	5.1E–5	14
metoprolol	267	4.8	1	7.4	1.20	–0.80	R	6.2E–5	14
nadolol	309	4.9	1	7.4	0.23	–1.77	R	5.3E–5	14
oxprenolol	265	4.7	1	7.4	1.69	–0.31	R	9.0E–6	14
pindolol	248	4.6	1	7.4	1.67	–0.33	R	1.5E–5	14
propranolol	259	4.7	1	7.4	2.75	0.75	R	2.0E–5	14
Sotalol	272	4.6	2	7.4	0.23	–1.47	R	6.8E–5	14
timolol	316	4.8	1	7.4	1.61	–0.39	R	5.2E–5	14
timolol	316	4.8	1	7.0	1.61	–0.39	R	1.3E–5*	33

[a] Molecular mass (or average molecular mass). [b] Percent of molecules nonionized at experimental pH. [c] Octanol–water partition coefficient, *P*. Partition coefficients were not calculated for macromolecules, since they are assumed not to partition into the lipid phase. [d] Octanol–water distribution coefficient, *D*, determined at experimental pH. [e] Source of tissue: rabbit (R). [f] All permeability measurements were made in vitro, except those followed by an asterix (*), which were made in vivo.

layers of cells each connected by tight junctions, which is expected to provide a large barrier to anything but small, lipophilic compounds. The stroma is a thick (450 μm), fibrous, largely acellular tissue composed mostly of water, which should not provide a lipophilic barrier. Finally, the endothelium is a monolayer of cells with large intercellular junctions, which should present a leaky lipophilic barrier.

The resistance to transport across the whole cornea can be thought of as a sum of resistances to transport across each of the individual corneal layers, where the resistance to transport (R) is the inverse of permeability (P):

$$R_{\text{cornea}} = R_{\text{epithelium}} + R_{\text{stroma}} + R_{\text{endothelium}}$$

$$\frac{1}{P_{\text{cornea}}} = \frac{1}{P_{\text{epithelium}}} + \frac{1}{P_{\text{stroma}}} + \frac{1}{P_{\text{endothelium}}}$$

Using this "sum of resistances" approach allows us to determine which layers of the cornea provide rate-limiting barriers by comparing the permeability of full cornea to the permeability of cornea with one or more of its layers removed. For example, if the permeability of full cornea was found to be smaller than that of de-epithelialized cornea, it would suggest that the epithelium presents a significant barrier to transport. In contrast, if the permeability of full cornea was found to be equal to that of de-epithelialized cornea, it would suggest that the epithelium

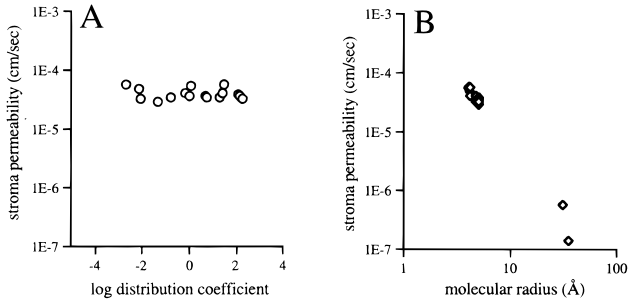

Figure 2—Permeability of corneal stroma. All data come from Table 2. Stroma permeability depends strongly on molecular radius and shows little dependence on distribution coefficient.

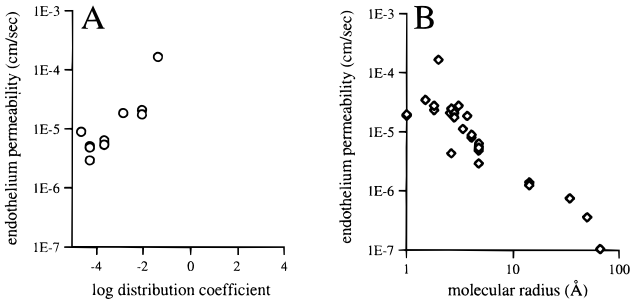

Figure 3—Permeability of corneal endothelium. All data come from Table 3. Endothelium permeability depends on both molecular radius and distribution coefficient.

does not present a significant barrier to transport. This type of analysis will be used throughout the remainder of this paper.

When the stromal layer of cornea is isolated, its permeability shows no apparent dependence on distribution coefficient and a strong dependence on molecular radius (Figure 2), as expected for its anatomical structure (i.e., hydrophilic and fibrous). Because whole cornea and corneal stroma have such different permeability properties, it at first appears that the stroma is not a rate-limiting barrier within the cornea. However, comparing the permeabilities for small compounds across the stroma (Figure 2A) and the full cornea (Figure 1A), the full range of stromal permeabilities falls within the upper range of corneal permeabilities (i.e., $K_p = 10^{-5}$ to 10^{-4} cm/s). This indicates that while the stroma may not limit compounds that show a small corneal permeability (e.g., hydrophilic compounds), the stroma provides a barrier to lipophilic compounds that is similar to that of the whole cornea. Stated another way, if a molecule is sufficiently lipophilic to readily cross the epithelium (and endothelium; i.e., $K_p > 10^{-5}$ cm/s), the barrier presented by stroma appears to become important. Thus, stroma is sometimes one of the rate-limiting layers.

The permeability of just the endothelial layer of cornea is shown in Figure 3 and displays a strong dependence on both distribution coefficient and molecular size. This indicates that both the lipophilic pathway across cells (related to distribution coefficient) and the hydrophilic pathway between cells (related to molecular size) are important. To determine if endothelium is a rate-limiting step for transport across the full cornea, the permeability of endothelium (Figure 3A) can be compared to that of the cornea (Figure 1A). For molecules with the same distribution coefficient, endothelial permeability is generally larger than that of cornea, which indicates that the endothelium is more permeable and, thus, not a rate-limiting barrier. Note, however, that the data available for endothelium are only for hydrophilic compounds, which are known to cross epithelium very poorly. It is therefore not clear from this

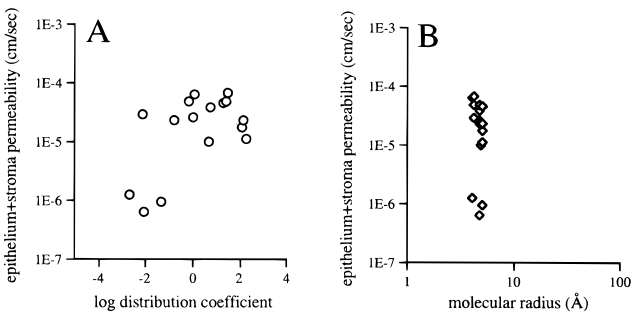

Figure 4—Permeability of corneal epithelium-plus-stroma. All data come from Table 4. Epithelium-plus-stroma permeability is a function of the distribution coefficient.

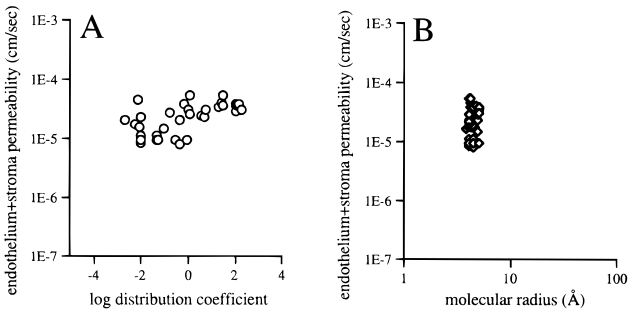

Figure 5—Permeability of corneal endothelium-plus-stroma. All data come from Table 5. Endothelium-plus-stroma permeability may be a function of the distribution coefficient.

data set whether endothelial barrier properties could be important for lipophilic compounds crossing the cornea.

To help answer this question, we can use another data set, which includes information largely on lipophilic compounds. Data on epithelium-plus-stroma (or de-endothelialized cornea) are shown in Figure 4. As a function of distribution coefficient, the values for permeability of de-endothelialized cornea follow the range of values for full cornea (Figure 1A), but permeability of de-endothelialized cornea tends toward higher permeabilities. Thus, this data set confirms that the endothelium is not uniquely rate-limiting, but suggests that it plays some role in the corneal barrier for lipophilic molecules.

The data thus far indicate that neither stroma nor endothelium is uniquely rate-limiting, but each can play a role in limiting transport of small, lipophilic compounds. By process of elimination, this leaves the epithelium as the dominant barrier in cornea. This indirect assertion could be verified by directly comparing permeability of epithelium to full cornea, but unfortunately, almost no permeability data exist in the literature for corneal epithelium alone. If we accept that epithelium dominates cornea's barrier properties, it still remains unclear which of the other layers (i.e., stroma and endothelium) is the second most important barrier.

One final set of data can help explain the relative roles of stroma versus endothelium. Figure 5 presents the permeability of endothelium-plus-stroma (or de-epithelialized cornea). The possible weak dependence on distribution coefficient suggests that endothelium influences the permeability of this composite tissue. Moreover, comparing Figures 2A and 3A shows that endothelial permeability is generally lower than that of stroma, further supporting the relative importance of endothelium. Similarly, comparing the permeability values shown in Figures 2B, 3B, and 5B shows that for small molecules (i.e., < 10 Å) the endothelium is less permeable. However, it appears from the limited data available in Figures 2B and 3B that the

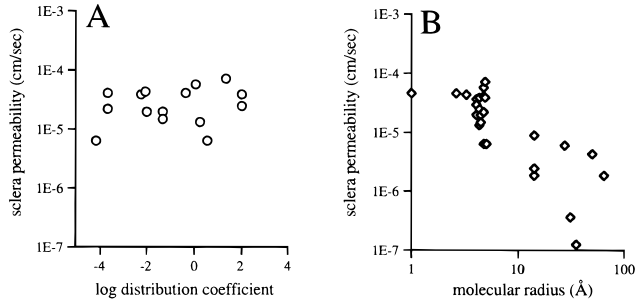

Figure 6—Permeability of sclera. All data come from Table 6. Sclera permeability depends strongly on molecular radius and shows no clear dependence on distribution coefficient.

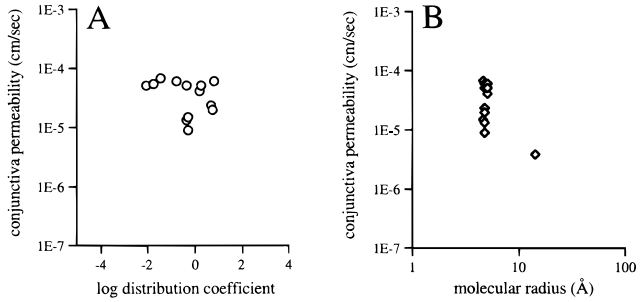

Figure 7—Permeability of conjunctiva. All data come from Table 7. Using this limited data set, conjunctiva permeability shows no clear dependence on molecular radius or distribution coefficient.

stromal permeability may be limiting for large compounds (i.e., > 10 Å).

To summarize the findings for cornea, this overall data set indicates that the epithelium is generally the rate-limiting barrier to transcorneal transport. Its barrier favorably depends on the lipophilicity of molecules and almost completely excludes macromolecules (r > 10 Å). For small molecules sufficiently lipophilic to readily cross epithelium ($K_p > 10^{-5}$ cm/s), the stroma and endothelium can play a significant role, where endothelium appears to be more important. For macromolecules, the stroma may provide a greater barrier than endothelium.

Permeability of Sclera and Conjunctiva—Scleral anatomy is similar to that of corneal stroma. Although the data are somewhat noisier for sclera, the permeability of sclera is also similar to that of stroma: no apparent dependence on distribution coefficient and a strong dependence on molecular radius (Figure 6). The relatively high scleral permeability, as compared to the cornea, has motivated some researchers to investigate transscleral drug delivery, especially for compounds that need to be administered locally to the back of the eye (e.g., the retina).[9,13]

On its external anterior surface, sclera is covered by conjunctiva, which is an epithelial tissue. The limited data available on conjunctiva show no clear dependence on distribution coefficient and a possible dependence on molecular size (Figure 7). One would expect conjunctival permeability to show a preference for lipophilic molecules, because it is a cellular tissue. Comparing to Figure 1, conjunctiva appears to have similar or greater permeability than cornea. Given that this graph (Figure 7) is based on only two studies (Table 7), one of which was performed in vivo, future studies should better clarify how conjunctiva permeability depends on solute physicochemical properties.

Conclusion

This study has compiled well over 300 data points for the permeability of ocular tissues. Analysis of these data yields conclusions about the nature of different ocular tissue barriers which are generally consistent with conclusions reached in the individual studies which make up the data set. We hope this database will serve as a useful vehicle for developing and validating future models, which will yield improved mechanistic understanding and predict rates of drug delivery to the eye.

References and Notes

1. Lang, J. C. Ocular drug delivery: Conventional ocular formulations. *Adv. Drug Deliv. Rev.* **1995**, *16*, 39.
2. Tasman, W. *Duane's Foundations of Clinical Ophthalmology*; Lippincott-Raven: Philadelphia, 1995.
3. Park, K. *Controlled Drug Delivery: Challenges and Strategies*; American Chemical Society: Washington, DC, 1997.
4. Kishida, K.; Otori, T. A quantitative study on the relationship between transcorneal permeability of drugs and their hydrophobicity. *Jpn. J. Ophthalmol.* **1980**, *24*, 251−259.
5. Schoenwald, R. D.; Huang, H.-S. Corneal penetration behavior of beta-blocking agents I: Physicochemical factors. *J. Pharm. Sci.* **1983**, *772*, 1266−1272.
6. Cooper, E. R.; Kasting, G. Transport across epithelial membranes. *J. Controlled Release* **1987**, *6*, 23−35.
7. Grass, G. M.; Cooper, E. R.; Robinson, J. R. Mechanisms of corneal drug penetration III: Modeling of molecular transport. *J. Pharm. Sci.* **1988**, *77*, 24−26.
8. Yoshida, F.; Topliss, J. G. Unified model for the corneal permeability of related and diverse compounds with respect to their physicochemical properties. *J. Pharm. Sci.* **1996**, *85*, 819−823.
9. Edwards, A.; Prausnitz, M. R. A fiber matrix model of sclera and corneal stroma for drug delivery to the eye. *AIChE J.* **1998**, *44*, 214−225.
10. Pearlman, R. S. In *Partition Coefficient Determination and Estimation*; Dunn, W. J., Block, J. H., Pearlman, R. S., Eds.; Pergamon Press: New York, 1986; pp 3−20.
11. Reid, R. C.; Prausnitz, J. M.; Poling, B. E. *The Properties of Gases and Liquids*; McGraw-Hill: New York, 1987.
12. Fatt, I.; Weissman, B. A. *Physiology of the Eye: An Introduction to the Vegetative Functions*; Butterworth-Heinemann: Boston, 1992.
13. Olsen, T. W.; Edelhauser, H. F.; Lim, J. I.; Geroski, D. H. Human scleral permeability: effects of age, cryotherapy, transscleral diode laser, and surgical thinning. *Invest. Ophthalmol. Vis. Sci.* **1995**, *36*, 1893−1903.
14. Wang, W.; Sasaki, H.; Chien, D.-S.; Lee, V. H. L. Lipophilicity influence on conjunctival drug penetration in the pigmented rabbit: a comparison with corneal penetration. *Curr. Eye Res.* **1991**, *10*, 571−579.
15. Huang, H.-S.; Schoenwald, R. D.; Lach, J. L. Corneal penetration behavior of beta-blocking agents II: Assessment of barrier contributions. *J. Pharm. Sci.* **1983**, *72*, 1272−1279.
16. Tang-Liu, D. D.-S.; Richman, J. B.; Weinkam, R. J.; Tarkruri, H. Effects of four penetration enhancers on corneal permeability of drugs in vitro. *J. Pharm. Sci* **1994**, *83*, 85−90.
17. Duffel, M. W.; Ing, I. S.; Segarra, T. M.; Dixson, J. A.; Barfnecht, C. F.; Schoenwald, R. D. N-Substituted sulfonamide carbonic anhydrase inhibitors with topical effects on intraocular pressure. *J. Med. Chem.* **1986**, *29*, 1488−1494.
18. Maren, T. H.; Jankowska, L.; Sanyal, G.; Edelhauser, H. F. The transcorneal permeability of sulfanomide carbonic anhydrase inhibitors and their effect on aqueous humor secretion. *Exp. Eye Res.* **1983**, *36*, 457−480.
19. Conroy, C.; Buck, R. Influence of ion pairing salts on the transcorneal permeability of ionized sulfonamides. *J. Ocular Pharmacol.* **1992**, *8*, 233−240.
20. Edelhauser, H. F.; Maren, T. H. Permeability of human cornea and sclera to sulfonamide carbonic anhydrase inhibitors. *Arch. Ophthalmol.* **1988**, *106*, 1110−1115.
21. Jankowska, L.; Bar-Ilan, A.; Maren, T. The relations between ionic and nonionic diffusion of sulfonamides across the rabbit cornea. *Invest. Ophthal. Vis. Sci.* **1986**, *27*, 29−37.
22. Grass, G. M.; Robinson, J. R. Mechanisms of corneal drug penetration I: In vivo and in vitro kinetics. *J. Pharm. Sci.* **1988**, *77*, 3−14.
23. Schoenwald, R. D. in *Controlled Drug Bioavailability*; Smolen, Ball, Eds.; Wiley & Sons: New York, 1985; pp 257−306.
24. Chiang, C.-H.; Schoenwald, R. D. Ocular pharmacokinetic models of clonidine-3H hydrochloride. *J. Pharmacokin. Biopharm.* **1986**, *14*, 175−211.
25. Chiang, C.-H.; Schoenwald, R. D.; Huang, H.-S. Corneal permeability of adrenergic agents potentially useful in glaucoma. *J. Taiwan Pharmaceut. Assoc.* **1986**, *38*, 67−84.

26. Igarashi, H.; Sato, Y.; Hamada, S.; Kawasaki, T. Studies on rabbit corneal permeability of local anesthetics. *Jpn. J. Pharmacol.* **1984**, *34*, 429−434.
27. Schoenwald, R. D.; Ward, R. L. Relationship between steroid permeability across excised rabbit cornea and octanol−water partition coefficients. *J. Pharm. Sci.* **1978**, *67*, 786−788.
28. Schoenwald, R. D.; Houseman, J. A. Disposition of cyclophosphamide in the rabbit and human cornea. *Biopharmaceut. Drug Disposition* **1982**, *3*, 231−241.
29. Schoenwald, R. D. Ocular drug delivery: Pharmacokinetic considerations. *Clin. Pharmacokinet.* **1990**, *18*, 255−269.
30. Eller, M. G.; Schoenwald, R. D.; Dixson, J. A.; Segarra, T.; Barfkneckt, C. F. Topical carbonic anhydrase inhibitors III: Opimization model for corneal penetraion of ethoxzolamide analogues. *J. Pharm. Sci.* **1985**, *74*, 155−160.
31. O'Brien, W. J.; Edelhauser, H. F. The corneal penetration of trifluorothymidine, adenine arabinoside, and idoxuridine: a comparative study. *Invest. Ophthal. Vis. Sci.* **1977**, *16*, 1093−1103.
32. Muchtar, S.; Abdulrazik, M.; Frucht-Pery, J.; Benita, S. Ex-vivo permeation study of indomethacin from a submicron emulsion through albino rabbit cornea. *J. Controlled Release* **1997**, *44*, 55−64.
33. Ahmed, I.; Gokhale, R. D.; Shah, M. V.; Patton, T. F. Physicochemical determinants of drug diffusion across the conjunctiva, sclera, and cornea. *J. Pharm. Sci.* **1987**, *76*, 583−587.
34. Suhonen, P.; Järvinen, T.; Peura, P.; Urtti, A. Permeability of pilocarpic acid diesters across albino rabbit cornea in vitro. *Int. J. Pharm.* **1991**, *74*, 221−228.
35. Siefert, B.; Keipert, S. Influence of alpha-cyclodextrin and hydroxyalkylated beta-cyclodextrin derivatives on the in vitro corneal uptake and permeation of aqueous pilocarpine-HCl solutions. *J. Pharm. Sci.* **1997**, *86*, 716−720.
36. Musson, D. G.; Bidgood, A. M.; Olejnik, O. An in vitro comparison of the permeability of prednisolone, prednisolone sodium phosphate, and prednisolone acetate across the NZW rabbit cornea. *J. Ocular Pharmacol.* **1992**, *8*, 139−149.
37. Wu, N.; Chiang, C.; Lee, A. Studies of carbonic anhydrase inhibitors: Physicochemical properties and bioactivities of new thiadiazole derivatives. *J. Ocular Pharmacol.* **1993**, *9*, 97−108.
38. Chang, S.-C.; Bundgaard, H.; Buur, A.; Lee, V. Improved corneal penetation of timolol by prodrugs as a means to reduce systemic drug load. *Invest. Ophthal. Vis. Sci.* **1987**, *28*, 487−491.
39. Maurice, D. M.; Watson, P. G. The distribution and movement of serum albumin in the cornea. *Exp. Eye Res.* **1965**, *4*, 355−363.
40. Maurice, D. M. The structure and transparency of the cornea. *J. Physiol.* **1957**, *136*, 263−286.
41. Allansmith, M.; de Ramus, A.; Maurice, D. The dynamics of IgG in the cornea. *Invest. Ophthal. Vis. Sci.* **1979**, *18*, 947−955.
42. Hale, P. N.; Maurice, D. M. Sugar transport across the corneal endothelium. *Exp. Eye Res.* **1969**, *8*, 205−215.
43. Riley, M. V. A study of the transfer of amino acids across the endothelium of the rabbit cornea. *Exp. Eye Res.* **1977**, *24*, 35−44.
44. Hodson, S.; Miller, F. The bicarbonate ion pump in the endothelium which regulates the hydration of rabbit cornea. *J. Physiol.* **1976**, *263*, 563−577.
45. Kim, J. H.; Green, K.; Martinez, M.; Paton, D. Solute permeability of the corneal endothelium and descemet's membrane. *Exp. Eye Res.* **1971**, *12*, 231−238.
46. Maurice, D. M. In *The Eye: Vegatative Physiology and Biochemistry*; Davidson, H., Ed.; Academic Press: Orlando, FL, 1984; pp 1−129.
47. Ota, Y.; Mishima, S.; Maurice, D. M. Endothelial permeability of the living cornea to fluorescein. *Invest. Ophthalmol. Vis. Sci.* **1974**, *13*, 945−949.
48. Mishima, S.; Trenberth, S. M. Permeability of the corneal endothelium to nonelectrolytes. *Invest. Ophthalmol.* **1968**, *7*, 34−43.
49. Maurice, D. M. The permeability to sodium ions of the living rabbit's cornea. *J. Physiol.* **1951**, *112*, 367−391.
50. Maurice, D. M.; Polgar, J. Diffusion across the sclera. *Exp. Eye Res.* **1977**, *25*, 577−582.
51. Hämäläinen, K. M.; Kontturi, K.; Auriola, S.; Murtomäki, L.; Urtti, A. Estimation of pore size and pore density of biomembranes from permeability measurements of polyethylene glycols using an effusion-like approach. *J. Controlled Release* **1997**, *49*, 97−104.

Acknowledgments

We thank Robert Pearlman, Butch Carreira, Sam Karickhoff and John Blankly for invaluable assistance in determining physical properties of drugs. We also thank Aurelie Edwards, Henry Edelhauser, Dayle Geroski and Shilpa Kaushik for helpful discussions. This work was supported in part by an NSF Career Young Investigator Award (BES-9624832) and the Emory/Georgia Tech Biomedical Technology Research Center.

JS9802594